ELSEVIER

European Journal of Pharmaceutical Sciences 14 (2001) 271–280

EUROPEAN JOURNAL OF PHARMACEUTICAL SCIENCES

www.elsevier.nl/locate/ejps

Drug absorption in vitro model: filter-immobilized artificial membranes 2. Studies of the permeability properties of lactones in *Piper methysticum* Forst ☆

Alex Avdeef[a,*], Melissa Strafford[a], Eric Block[b], Michael P. Balogh[b], Walter Chambliss[c], Ikhlas Khan[d]

[a] *pION Inc., 5 Constitution Way, Woburn, MA 01801, USA*
[b] *Waters Corporation, 34 Maple Street, Milford, MA 01757-3696, USA*
[c] *National Center for Natural Products Research and the Department of Pharmaceutics, School of Pharmacy, University of Mississippi, University, MS 38677, USA*
[d] *National Center for Natural Products Research and the Department of Pharmacognosy, School of Pharmacy, University of Mississippi, University, MS 38677, USA*

Received 2 February 2001; received in revised form 28 June 2001; accepted 4 July 2001

Abstract

The assessment of transport properties of 23 drug and natural product molecules was made using the in vitro model based on filter-immobilized artificial membranes (filter-IAM), assembled from phosphatidylcholine in dodecane, in buffer solutions at pH 7.4. Five of the compounds were lactones extracted from the roots of the kava-kava plant. Experiments were designed to test the effects of stirring (0–600 rpm) during assays and the effects of varying the assay times (2–15 h). The highly mobile kava lactones permeated in the order dihydromethisticin (40)>yangonin (37)>kavain (34)>methisticin (32)>desmethoxyyangonin (26), the numbers in parentheses being the measured effective permeabilities in units of 10^{-6} cm/s. By comparison, commercial drugs ranked: phenazopyridine (35)>testosterone (19)>propranolol (13)>ketoconazole (6.3)>piroxicam (2.2)>caffeine (1.7)>metoprolol (0.8)>terbutaline (0.01). In addition to permeability measurements, membrane retention of compounds was determined. Yangonin, desmethoxyyangonin, ketoconazole, and phenazopyridine were more than 60% retained by the artificial membranes containing phospholipids. Stirring during assay significantly increased the observed permeabilities for highly mobile molecules, but had minimal impact on the poorly permeable molecules. The influence of hydrogen bonding was explored by determining permeabilities using filters coated with dodecane free of phospholipids. In the filter-IAM method, concentrations were determined by microtitre plate UV spectrophotometry and by LC–MS. Higher-throughput was achieved with direct UV by the use of 96-well microtitre plate formats and with LC–MS by the use of cassette dosing (five-in-one).

Keywords: Permeability; Absorption; Parallel artificial membrane permeability assay (PAMPA); Filter-immobilized artificial membranes (filter-IAM); Cassette dosing; Liquid chromatography–mass spectrometry (LC–MS)

1. Introduction

The competitive pressure in pharmaceutical research laboratories to lower the attrition rates of development compounds has spurred the introduction of new high-throughput instrumental methods to screen for bio-pharmaceutical properties early in the drug discovery stage. In this context, the new membrane permeability in vitro assay, called PAMPA, has attracted considerable attention (Kansy et al., 1998). An extended version of the method, called filter-immobilized artificial membranes (filter-IAM) permeability assay, has been recently described (Avdeef, 2001). The latter technique is further evolved in the present study, with an application featuring highly-permeable natural product molecules derived from the kava-kava plant.

The extracts from the roots of the kava-kava plant, a member of the pepper family (‘kava’ is the common name for the botanical species *Piper methysticum* Forst, and also refers to the psychoactive beverage made from it), appear to possess relaxing and mildly euphoric effects (Furgiuele

☆ Ref. Avdeef, 2001 is Part I of the series.

*Corresponding author. Tel.: +1-781-935-8939; fax: +1-781-935-8938.

E-mail address: aavdeef@pion-inc.com (A. Avdeef).

0928-0987/01/$ – see front matter
PII: S0928-0987(01)00191-9

et al., 1965; Kilham, 1996). The plant is a perennial shrub distributed and cultivated on the Pacific islands of Polynesia and Micronesia (Singh, 1992). The pharmacologically active constituents of kava extracts are known to be lactones; more than a dozen have been identified to date (Holm et al., 1991; Backhaub and Krieglstein, 1992; Leung and Foster, 1996). The six dominant lactones (**1**–**6**) account for ~30% of the extract weight. There are kava-based drugs on the market in Germany (Bruneton, 1995). However, kava products in the USA are regulated as dietary supplements, and are not held to strict quality control standards like drug products. It is possible to purchase tablets of kava extract (70–200-mg usage level) in health food stores and over the internet (www.internet-nutrition.com/topics/kavakava.html). Since the kava plants from various origins show significant quantitative and qualitative differences, it is important to have efficient analytical methods in manufacturing, in order to ensure product quality and safety. To that end, methods based on HPLC have been highly refined (Ganzera and Khan, 1999).

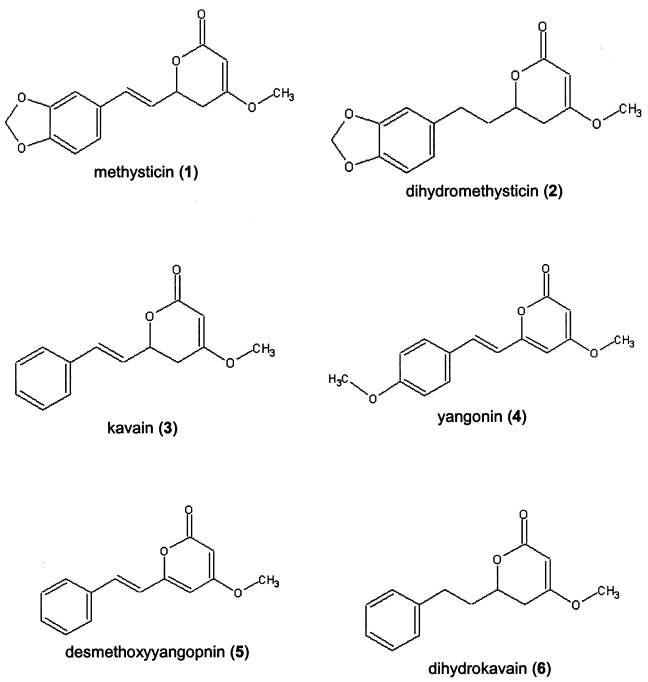

The present study examined the membrane transport properties of five of the lactones (**1**–**5**), along with coumarin, testosterone, and phenazopyridine, as well as a number of commercial drugs with unrelated structures, ranging over four orders of magnitude in permeability. Phosphatidylcholine dodecane solutions were deposited on filters under conditions where bilayers are expected to form (Thompson et al., 1982). The transport properties of some of the compounds were also examined using filters coated with phospholipid-free dodecane. Since preliminary filter-IAM measurements of kava lactones indicated highly permeable compounds, these compounds were selected to study in detail the effect of stirring, permeation times, and cassette dosing in the filter-IAM methodology.

The filter-IAM technique was used to process well-purified samples. In addition, individual kava lactones were combined in a cassette sample. Permeability rates were then derived by both direct UV spectrophotometric measurements and LC–MS analysis. As the results from UV detection can be skewed by the presence of contaminants and impurities, LC–MS detection was investigated due to its inherent sensitivity and specificity. Since, in the analysis of combinatorial libraries by high-throughput methods it is impractical to optimize HPLC and MS conditions for every compound, this study made use of generic chromatographic and mass spectrophotometric conditions.

2. Materials and methods

2.1. Materials

All kava lactones were isolated at the National Center for Natural Products Research; identity and purity were confirmed by chromatographic means (TLC, HPLC, GC) and NMR (^{1}H and ^{13}C). 1,2-Dioleoyl-sn-glycero-3-phosphocholine was purchased as a high-purity powder from Avanti Polar-Lipids (Alabaster, AL, USA), and was stored at −20°C when not used. Spectroscopic grade dodecane was purchased from EM Science (Gibbstown, NJ, USA). Spectroscopic grade dimethylsulfoxide was purchased from Burdick and Jackson (Muskegon, MI, USA). Amitriptyline hydrochloride, caffeine, corticosterone, coumarin, desipramine hydrochloride, diltiazem hydrochloride, erythromycin, furosemide, ibuprofen, ketoconazole, metoprolol tartrate, oxprenolol, phenazopyridine hydrochloride, piroxicam, propranolol hydrochloride, terbutaline hemisulfate, testosterone, and verapamil hydrochloride were purchased from Sigma–Aldrich (St. Louis, MO, USA). The pH of the assayed solutions was adjusted with a universal buffer (PN 100621, *p*ION). HPLC–MS analysis used reverse-osmosis deionized water from a Milli-Q Gradient system (Millipore, Bedford, MA, USA), HPLC-grade acetonitrile (JT Baker), and reagent-grade ammonium acetate (Sigma, St. Louis, MO, USA).

2.2. Filter-IAM permeabilty method

In the filter-IAM assay, a ‘sandwich’ is formed from a 96-well microtitre plate and a 96-well filter plate, such that each composite well (schematically represented in Fig. 1) is divided into two chambers: donor at the bottom and acceptor at the top, separated by a 125-μm microfilter disc (0.45-μm pores), coated with a 2% (w/v) dodecane solution of dioleoylphosphatidylcholine, under conditions that multilamellar bilayers form inside the filter channels

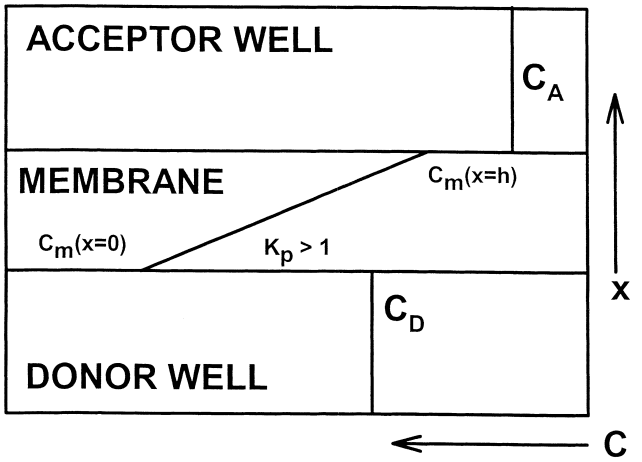

Fig. 1. Schematic of the three-component steady-state transport model, where a lipophilic sample (with partition coefficient, $K_p > 1$), introduced in the donor well, is at concentration C_D. The concentration of the sample in the acceptor well is C_A. The concentration of the sample in the membrane, C_m, is position dependent, having a maximum value at the donor–membrane interface and a minimum value at acceptor–membrane interface. The concentration gradient in the membrane, dC_m/dx, is linear at steady-state, and is proportional to the partition coefficient.

when the system contacts an aqueous buffer solution (Thompson et al., 1982).

2.3. Transport model and its dependence on permeability, solubility and pH

Fick's first law applied to homogeneous membranes at steady state (Weiss, 1996) may be stated as

$$J = D_m\, dC_m/dx = D_m[C_m(0) - C_m(h)]/h \quad (1)$$

where J is the flux, in units of mol cm^{-2} s^{-1}, $C_m(0)$ and $C_m(h)$ are the concentrations, in mol cm^{-3} units, of solute within the membrane at the two water–membrane interfaces (at positions $x = 0$ and $x = h$ (Fig. 1), where h is the thickness of the membrane in cm units), and D_m is the diffusivity of the solute within the membrane, in units of cm^2 s^{-1}. At steady state, the concentration gradient, dC_m/dx, within the membrane is linear, hence the difference may be used in the right side of Eq. (1).

Since one can estimate (or possibly measure) the distribution coefficients between bulk water and the membrane, K_p, one can convert Eq. (1) into a more practical form,

$$J = D_m K_p (C_D - C_A)/h \quad (2)$$

where the substitution of K_p allows one to use bulk water concentrations in the donor and acceptor compartments, C_D and C_A, respectively (Fig. 1). These concentrations may be readily measured by standard techniques. In a further simplification, it is a common practice to combine the three constants into one composite parameter, called 'effective permeability', P_e,

$$P_e = D_m K_p / h \quad (3)$$

The relevance of Eq. (2) (which predicts how quickly molecules pass through a membrane) to solubility comes in the concentration terms. Consider 'sink' conditions, where C_A is essentially zero, as would be the case on the basolateral side of the epithelial cell barrier in the small intestine: Eq. (2) reduces to the following simplified flux expression

$$J = P_e C_D \quad (4)$$

Flux depends on the product of effective permeability of the solute (which we may presume to be most likely the uncharged, unaggregated molecular species) times the concentration of the species at the water-side of the donor surface of the membrane. This concentration ideally may be equal to the dose of the drug, unless the dose exceeds the solubility limit, in which case it is equal to the solubility. If only the uncharged molecular species permeates appreciably, then Eq. (4) may be restated as

$$J = P_0 C_0 \le P_0 S_0 \quad (5)$$

where P_0 and C_0 are the intrinsic permeability and concentration of the uncharged species, respectively. The intrinsic permeability does not depend on pH, but its cofactor in the flux equation, C_0, does (for ionizable molecules). The concentration of the uncharged species is equal to or less than the intrinsic solubility of the species, S_0.

Effective permeability, P_e, can be deduced in several ways, depending on experimental design and specific assumptions made. In permeability measurements using monolayers of cultured colonic cancer cells, Caco-2, it is customary to use the expression (Sawada et al., 1999)

$$P_{e=} V_D/(A M_D(0))(\Delta M_A/\Delta t) \quad (6)$$

where V_D is the donor well volume (0.2–0.4 cm^3), A is the filter area (0.3 cm^2), $M_D(0)$ is the sample amount (mol) in the donor well at the start of the assay (time = 0), and ΔM_A is the amount of sample transferred to the acceptor compartment (but removed to maintain sink conditions) after an interval of time, Δt (in s). $\Delta M_A/\Delta t$ is determined as the slope of the plot of M_A vs. t, evaluated after steady state is reached. This is the so-called the 'one-way flux' formula, which is valid under sink conditions.

If sink conditions are not maintained, the 'two-way flux' equation is more complicated (Palm et al., 1999),

$$C_A(t) = M/(V_D + V_A) + (C_A(0) - M/(V_D + V_A))\exp\{-P_e A(1/V_D + 1/V_A)t\} \quad (7)$$

where M refers to the total amount (mol) of the drug in the system, $C_A(t)$ is the concentration of the drug (mol/cm^3) in the acceptor well at time t, and V_A is the volume of the acceptor well (0.2–0.4 cm^3).

2.4. Retention of compounds by the membrane

Eqs. (6) and (7) do not explicitly consider the effect of mass loss to the membrane (or cell monolayer). The equation used in the present study is a modified version of Eq. (7), where the total amount is not M, but M minus the amount of sample lost to the membrane.

Acceptor and donor concentrations are measured at two time points in the filter-IAM method: at $t = 0$ and $t = 2–15$ h (permeation time). It is assumed that the time to reach steady state is short relative to the total permeation time. In the limit of very vigorous stirring, the time to saturate the membrane with sample and reach the steady state is estimated to be ~10 s (Weiss, 1996). With unstirred plates, however, typical times to saturated membranes are ~20 min (unpublished data). For highly permeable compounds (octanol–water log $D > 3$), if the microtitre plate solutions are not stirred and the permeation time is short, the permeability constant calculated from Eq. (7) is underestimated.

The membrane retention can be substantial with lipophilic compounds, as much as 40–90% in some Caco-2 studies (Wils et al., 1994; Sawada et al., 1999). By modifying M in Eq. (7) for material lost to the membranes, our transport model equation accounts for the disposition of the entire mass. In the present study, the mass lost to the membrane is estimated by measuring both the acceptor and the donor well sample amounts, and assuming that any amount less than the total mass introduced at the start is lost to the membrane. The assumption has been validated by control measurements, where the filters were not coated by the lipid solution (unpublished data). The membrane retention, R, is expressed as a mol% in this study.

2.5. Permeability instrument with direct UV detection

The PSR4p instrument (*p*ION) was used in this study. Samples are typically introduced as 10 mM DMSO solutions in a 96-well polypropylene microtitre plate. The robotic liquid handling system (Tecan, Research Triangle Park, NC, USA) draws a 3–10-μl aliquot of the DMSO solution and mixes it into an aqueous buffer solution, so that the final typical sample concentrations are 5–150 μM and the DMSO concentrations are <2% (v/v). The solutions are agitated on an orbital shaker for 2–5 h, or are allowed to stand for 6–15 h without shaking, and assayed by direct UV spectrophotometry, in the 200–500-nm domain.

When shaken, the microtitre plate 'sandwich' was covered with a plastic lid and clamped securely, to avoid separation of the two plates. The four-position plate shaker had a circular pattern of motion, whose frequency was calibrated carefully. The top-compartment liquid did not splash against the lid at speeds as high as 600 rpm.

When plastic UV plates are used, only the data above 240 nm are used in analysis. The direct UV measurement eliminates the need for method development and easily lends itself to more complete automation, hence, significantly higher throughput than simple chromatographic techniques is achieved.

The buffers used in the assay are automatically prepared by the PSR4p robotic system. The quality controls of the buffers and the pH electrode are performed by alkalimetric titration, incorporating the procedure of Avdeef and Bucher (1978). Following the completion of the UV assays, the pH in each microtitre plate well was measured to confirm proper value.

2.6. Permeability determination by LC–MS

Separation was performed with an Alliance® HT HPLC system (Waters, Milford, MA, USA), using a 2.1×20-mm XTerra® column (2.6 μm, Waters). Column flow was split with a zero dead-volume 'T' union (Upchurch Scientific, Oak Harbor, WA, USA); ~90% of flow went to a model 996 UV photodiode array detector (Waters); the remainder was directed to a ZMD® single quadrupole mass spectrometer (Waters).

Data acquisition and reduction utilized the MassLynx™ software package (Micromass, Manchester, UK). Automated data reduction and reporting was performed with the OpenLynx™ software module. Chromatographic peak areas were integrated and used to derive permeability coefficients using the algorithms employed by the PSR4p software. Table 1 lists the instrumental conditions used in this study.

Table 1
LC–MS instrumental conditions

HPLC				
Column	2.1×30-mm Xterra C_{18} 2.5 μm			
Mobile phase	A	5% CH_3CN in H_2O (10 mM NH_4OAc)		
	B	90% CH_3CN in H_2O (10 mM NH_4OAc)		
Flow rate	1 ml/min			
Injection volume	5 μl			
Gradient	Time (min)	%A	%B	Gradient
	0	95	5	–
	3	0	100	8
	3.5	95	5	11
Mass spectrometer				
Mode	Alternating±ESI			
Scan range	100–500 amu			
Scan rate	0.3 s/scan			
Interscan time	0.2 s			
Capillary voltage	3600 V			
Source temp.	150°C			
Desolvation gas	240°C			
Cone voltage	24 V			

3. Results

3.1. Predictions of properties related to transport

Table 2 lists the physical properties of the kava lactones and the other molecules of focus. Included are the predicted partition coefficients, aqueous solubilities, blood–brain barrier ratios, and hydrogen-bonding factors, using three different commercial predictions software programs: ACD (Advanced Chemistry Development, Toronto, Canada; www.acdlabs.com), ABSOLV (Sirius Analytical Instruments, Forest Row, E. Sussex, UK; www.sirius-analytical.com; Abraham et al., 1994), and HYBOTPLUS (www.ibmh.msk.su/qsar/molpro; Raevsky et al., 2000). (The UNIX version of ABSOLV was used in this study.)

The kava lactones and the other three molecules in Table 2 have relatively weak hydrogen-bond accepting groups, as predicted by HYBOTPLUS. Testosterone has a weak hydrogen-bond donating group, and phenazopyridine has about twice as much hydrogen-bond donating tendency as testosterone. The kava lactones and coumarin lack hydrogen-bond donors. These hydrogen-bond properties were expected to impact on the measured permeabilities.

The predicted water solubilities were not useful in preparing stock solution plates: the kava compounds appeared to be much less soluble than predicted. Stock plates of the kava compounds could not be prepared even in DMSO, due to poor solubilities in that solvent. Methanol proved to be a useful solvent in the end. The actual solvent ratios (DMSO:methanol:water) used in the study are listed in Table 2.

3.2. Permeability by UV detection

Table 3 contains the pH 7.4 permeability results of the eight compounds of focus, based on experiments performed with different permeation times (2–15 h), different plate stirring rates (0–600 rpm), and two different lipid

Table 2
Physical properties

Compound	MW	Stock conc. (mM)	Stock % DMSO MeOH H_2O	Max peak (nm)	ΣC_a[a] ΣC_d[b]	Calc. log P[c]	Calc. S[d] (mg/ml)	Calc. log BBB[e]
Methysticin	274.3	5.5	25 50 25	265 305	2.35 0	1.51	79	−0.53
Dihydromethysticin	276.3	7.3	0 67 33	283 360	2.20 0	1.81	51	−0.43
Kavain	230.3	6.5	25 50 25	246	2.29 0	1.65	0.3	0.03
Yangonin	258.3	8.8	0 88 12	352 260	2.48 0	1.99	0.2	0.28
Desmethoxyyangonin	228.2	6.6	25 50 25	342 256	2.43 0	2.05	0.1	0.33
Coumarin	146.2	30	100 0 0	278 310	2.17 0	1.39	3	0.01
Testosterone	288.3	31	100 0 0	249	3.82 −2.11	3.48	0.007	0.03
Phenazopyridine	213.2	30	100 0 0	426 278	5.27 −5.04	2.55	0.2	−0.61

[a] Sum of hydrogen bond acceptor factors, calculated with HYBOTPLUS program.
[b] Calculated sum of hydrogen bond donor factors.
[c] Octanol–water partition coefficient, calculated with ACD program.
[d] Calculated aqueous solubility of the uncharged species, using ABSOLV program.
[e] Calculated logarithm of the ratio of substance in the brain–blood barrier, using ABSOLV.

Table 3
Permeability and retention at pH 7.4 and various permeation times, stirring speeds and lipid compositions[a]

Case	1a	1b	2a	2b	2c	2d	3a	3b	4a	4b	5a Dodecane	5b Dodecane
Time (h)	15.0	6.3	2.1	2.1	2.3	2.3	3.2	3.2	5.0	4.0	15.7	2.2
Stirring (rpm)	0	0	380	450	490	600	450	500	450	500	0	490
Compound												
Methysticin	15.7[b]±2.9[c]	32.1±2.2	21.9±7.4	12.1±3.5	25.5±6.3	57.4±15.2	26.8±3.3	35.0±6.7	26.3±4.4	39.1±5.3	equ[e]	22.3±4.7
	65%[d]	50%	49%	35%	48%	44%	42%	60%	53%	55%	69%	48%
Dihydromethysticin	19.7±5.5	39.5±4.0	13.9±4.9	13.4±2.3	30.1±3.8	84.8±35.6	26.4±4.2	30.6±5.4	30.3±7.1	55.0±24.6	equ	28.5±4.0
	56%	42%	32%	28%	40%	36%	34%	53%	43%	51%	62%	33%
Kavain	15.1±3.5	34.4±4.0	13.9±6.5	13.1±1.4	26.5±2.5	69.1±21.0	23.1±4.9	33.3±6.4	25.3±4.1	30.1±7.6	21.9±2.4	25.0±2.1
	57%	43%	33%	29%	41%	42%	36%	49%	44%	46%	58%	36%
Yangonin	11.0±0.8	36.5±8.8	12.8±4.3	11.8±1.4	20.9±4.5	70.5±48.6	21.0±3.6	39.8±9.4	17.9±7.6	24.8±9.4	5.8±1.7	15.8±2.4
	85%	70%	67%	59%	67%	63%	56%	73%	68%	75%	76%	61%
Desmethoxyyangonin	12.6±0.9	25.7±7.0	9.8±5.3	9.9±0.6	19.3±3.6	68.1±37.4	15.2±3.4	28.2±7.7	16.4±5.9	26.1±15.5	16.2±0.5	16.9±4.8
	80%	72%	53%	53%	65%	70%	56%	72%	66%	69%	79%	57%
Coumarin	16.0±6.3	42.2±3.0	27.6±5.7	26.9±1.3	42.1±6.2	95.9±36.0	36.7±8.5	45.4±5.6	34.4±6.3	37.8±9.0	36.1±1.1	40.3±5.0
	12%	23%	21%	24%	23%	24%	21%	20%	22%	26%	19%	23%
Testosterone	11.3±0.6	19.3±3.6	19.1±4.8	17.2±1.0	29.4±3.1	70.0±20.2	29.0±4.5	34.2±4.0	24.9±3.6	25.4±5.9	21.3±0.4	28.5±1.7
	11%	16%	17%	16%	21%	17%	16%	17%	19%	18%	11%	10%
Phenazopyridine	32.2±2.7	34.9±3.0	5.7±1.8	8.8±1.9	18.5±2.7	58.8±33.3	17.3±1.3	27.4±3.3	24.9±8.4	18.8±14.5		39.4±5.2
	67%	69%	62%	54%	64%	68%	54%	71%	60%	71%		30%

[a] Microfilters were coated with DOPC-dodecane solution, except for cases 5, where only dodecane was used.
[b] Effective permeability in 10^{-6} cm/s units.
[c] Standard deviation in effective permeability, based on six replicates on one plate.
[d] Mass retained by the membrane/total mass×100%.
[e] Equilibrated: concentrations in acceptor wells equal to those in donor wells after the 15.7-h permeation time.

formulations (alkane with and without phospholipid additive). All eight compounds shown are highly permeable, but as can be seen, the results obtained depend on the protocol used. However, rank order is not strongly dependent on the protocol.

The 15 h-without-stirring protocol (case 1a, Table 3), originally favored by the Roche group (Kansy et al., 1998), appears to be too long for the most permeable molecules studied here. The common problem encountered was that at the end of 15 h, many of the wells were equilibrated (data not shown), hence it was not possible to determine kinetic parameters. One could assert that the compounds were highly permeable (which may be sufficient for screening purposes). The small differences between equilibrated concentrations and those near equilibration had large impacts on the calculated permeabilities. The numbers derived from the near-equilibrated state significantly underestimated the true effective permeabilities (case 1a). When the permeation time was reduced to 6 h, still without stirring (case 1b), larger effective permeabilities were determined for the highly-permeable molecules. These (case 1b) are apparently our most reliable estimates of the permeabilities.

We studied the consequences of choosing shorter permeation times and various levels of stirring of the sandwich plates during the permeation pause. Cases 2a–2d list the results of 2-h permeation times, with stirring taken from 380 to 600 rpm. In most cases, the derived permeabilities were significantly lower than those of the 'benchmark' case 1b. The steepest dependency on the stirring rate was indicated by phenazopyridine, the molecule with the highest amount of hydrogen-bond capacity (Table 2). The standard deviations at 600 rpm were exceptionally high (Fig. 2). In one case, the data (not shown) indicated that the lipid was largely detached from the filter support at 600 rpm.

Longer permeation times with stirring were explored in cases 3 and 4. In cases 5, the filters were coated with dodecane only. In the phospholipid-free preparations, phenazopyridine indicated near-benchmark values of permeability with only 2-h permeation times.

Fig. 2 shows bar graphs of the various conditions of stirring explored. The effective permeabilities increased with increased stirring; still the ranking of effective permeabilities among the molecules was largely preserved. It is quite apparent that the ratio of the testosterone-to-phenazopyridine bars dramatically decreased with increasing agitation. Phenazopyridine is more permeable than testosterone under these ideal experimental conditions.

3.3. Membrane retention

Table 3 lists the percentages of each compound retained by the membranes after the permeation time elapsed.

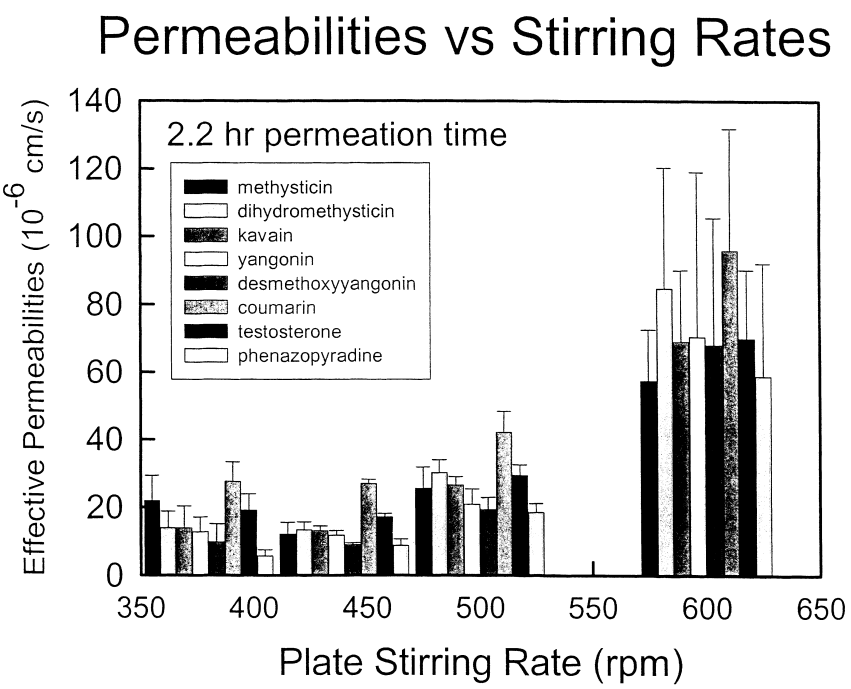

Fig. 2. Effective permeabilities of several compounds as a function of the stirring speed.

Yangonin, desmethoxyyangonin, and phenazopyridine exhibited retentions as high as 70–85%. High retentions have been reported for highly-lipophilic (octanol–water $\log D_{7.4} > 3$) compounds with Caco-2 monolayers. Retention in Caco-2 assays may be more of a problem than suggested by original publications. A recent examination (Rothen-Rutishauser et al., 2000) of the structures of the Caco-2 layers on filter supports, using laser-scanning confocal microscopy, indicates that under certain common conditions, multiple layers of cells can form on the filter. Such conditions would lead to further cell retention of lipophilic drugs. It is apparent in Table 3 that retentions do not appreciably depend on stirring and permeation time. However, the absence of phospholipid in the membranes dramatically lowered the retention of phenazopyridine (case 5b).

3.4. Comparison of LC–MS- and UV-derived permeability rates

Table 4 lists the permeabilities (UV- and LC–MS-based) of the compounds examined. Of the 23 compounds examined, only one failed to provide strong pseudomolecular ions by positive and/or negative electrospray ionization, suggesting that this approach should be appropriate to the analysis of combinatorial libraries. As may be seen, there is good parity between the two different analytical systems. The greater variation in the LC–MS is not surprising, since it includes variability incurred in sampling, chromatography and mass spectrometric response. Fig. 3 is a plot of UV- versus LC–MS-derived values. There is excellent correlation between the two data sets ($r^2 = 0.93$)

Table 4
Comparison of the effective permeabilities (pH 7.4) derived from LC–MS data with those derived by direct UV spectrophotometry[a]

Compound	P_e (10^{-6} cm/s), LC–MS	P_e (10^{-6} cm/s), UV	% R[b]
Methysticin	35.0±11.1	32.1±2.2	50
Dihydromethisticin	44.7±11.9	39.5±4.0	42
Kavain	31.4±12.5	34.4±4.0	43
Yangonin	43.4±16.6	36.5±8.8	70
Desmethoxyyangonin	23.4±6.9	25.7±7.0	72
Amitriptyline	16.0	9.3±4.1	53
Caffeine	1.8±0.7	1.73±0.04	1
Corticosterone	2.4±0.4	4.3±0.1	8
Coumarin	34.7±8.2	42.2±3.0	23
Desipramine	31.3±9.0	25.6±0.9	13
Diltiazem	13.6	18.6±4.6	21
Erythromycin	0.1	ND[c]	ND
Furosemide	ND	0.36±0.01 (0.071±0.006)[d]	3
Ibubrofen	3.2±0.3	1.9±0.4	0
Ketoconazole	6.2±1.0	6.3±0.4	62
Metoprolol	0.87±0.05	0.84±0.05	0
Oxprenolol	2.4	1.26±0.03	5
Phenazopyridine	29.4±1.7	34.9±3.0	69
Piroxicam	2.3±0.5	2.19±0.05	2
Propranolol	14.2±3.3	13.6±0.8	13
Terbutaline	0.06±0.02	0.40±0.03 (0.011±0.005)[d]	1
Testosterone	22.0	19.3±3.6	16
Verapamil	26.2±9.9	16.4±1.3	33

[a] No stirring; 6.3-h permeation time.
[b] Fraction of the compound retained by the filter-immobilized artificial membranes, as determined by the PSR4 instrument.
[c] Not detected.
[d] Freshly-prepared DMSO stock solution.

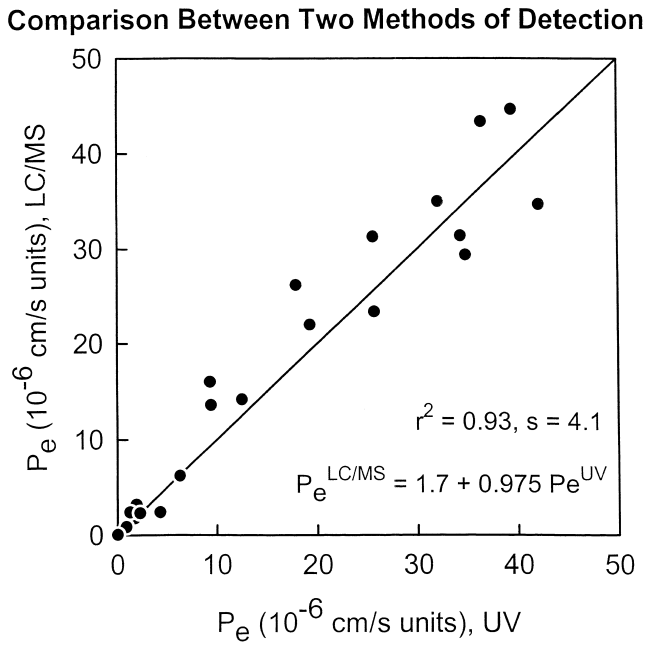

Fig. 3. Correlation between effective permeabilities determined by LC–MS and direct UV spectrophotometry.

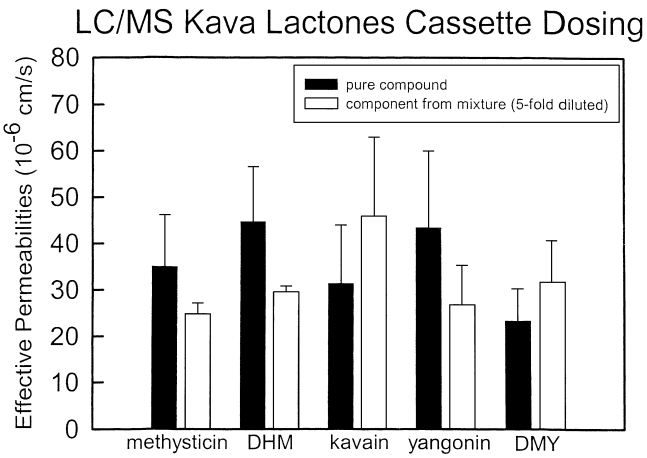

Fig. 4. Comparison of the permeabilities determined for pure kava lactones by direct UV spectrophotometry (black bars) and the permeabilities determined by LC–MS of an equimolar mixture of the five components (unfilled bars).

despite the fundamental differences between the two analytical methods.

3.5. Analysis of mixtures

The results discussed above were obtained from relatively pure compounds. In practice however, combinatorial library compounds at best have sample purity of 90–95%; values as low as 60% are not uncommon. Direct UV measurements represent the combined absorbance of all components in a given well. Impurities such as unreacted starting material, side-products and degradants sometimes can skew the UV-derived values. Because of the combination of chromatographic separation, coupled with the orthogonal mass spectrometric data, the components of mixtures can be quantified as discrete entities. This capability can be exploited in the analysis of '*n*-in-one' samples ('cassette dosing'). In this experiment, the five kava lactones were combined and processed in replicate; the LC–MS-derived values compared favorably with those obtained from individual standards, as can be noted in Fig. 4. While the mixture values track the individuals rather well, there is some significant difference in the values for any given compound. This discrepancy is due to experimental problems encountered during the analysis of the last few replicate samples. In this cassette-dosing example, individual permeability values cannot be determined by direct UV measurement. However, the PSR4p UV analysis of the mixture spectra clearly indicated the presence of multiple species, as indicated by the donor-well and acceptor-well peak manifold distortions due to differences in permeabilities of the individual compounds, in comparison to the peak shape of the manifold at the start of the permeation assay.

3.6. Confirmation of molecular weights and characterization of impurities

Because the mass spectrometer was operated in the full scan mode, molecular weight information was collected in the course of analysis. The use of alternating positive and negative ionization provided additional molecular weight confirmation. This confirmation was automated in the form of the MassLynx software module 'OpenLynx'. Acceptor wells corresponding to furosemide and terbutaline indicated that the expected weight was not supported by the mass spectral information collected. Since the corresponding wells in the donor and reference plates confirmed the molecular weights for these compounds, it would appear that little of these two compounds diffused across the membrane to the acceptor well. In the case of furosemide, the PSR4p UV analysis indicated that an impurity was present. However, the nature and cause of the impurity could not be readily determined from examination of the UV data. The terbutaline UV spectra did not directly indicate decomposition.

To confirm that decomposition was due to air exposure in the numerous freeze-and-thaw cycles of the DMSO stock solutions, fresh solutions were prepared for furosemide and terbutaline. Repeated UV analyses indicated lower permeabilities and the apparent absence of impurities for the two compounds (Table 4).

4. Discussion

We selected a series of highly-permeable natural product molecules to stage further development and exploration of

the new filter-IAM method for determining permeability of drug-like substances, to address the effect of hydrogen bonding on permeability, and to demonstrate the usefulness of the LC–MS method of detection in the filter-IAM methodology.

We were able to demonstrate that the permeation time could be lowered significantly below the 15-h value suggested in the original Roche publication (Kansy et al., 1998). For moderate to high permeability molecules, the best permeation time was found to be ~6 h, if stirring of the sandwich plate assembly were not done.

With stirring, the permeation time can be lowered to ~2 h. The short-time results are significantly of poorer quality, compared to those of the unstirred case. Stirring in excess of 600 rpm caused membrane coatings to detach, and is thus not recommended. Also, there was some well-position dependency of the result. Stirring is known to decrease the thickness of the unstirred water layer, leading to higher observed permeability of permeable compounds (Palm et al., 1999). It was observed that permeabilities derived from wells near the center of the microtitre plate were lower than values obtained from wells in the corners of the microtitre plate, an effect consistent with non-uniform stirring efficiency. For high-throughput screening applications, the benefit of reduced assay time may still outweigh the detrimental effects of stirring anisotropy.

The comparison of transport properties of phenazopyridine (strong hydrogen-bond donor), testosterone (mild hydrogen-bond donor), and the kava lactones (no hydrogen-bond donor groups), as indicated by cases 1 and 5 in Table 3, suggests that membrane retention is increased and permeability is decreased by hydrogen-bond donor groups. The membrane transport of phenazopyridine is about twice as fast and retention is about twice reduced in the inert lipid membranes compared to phospholipid-based membranes. Presumably the carbonyl groups in phospholipid components of the membrane strongly interact with molecules possessing hydrogen-bond donor groups.

It is interesting to note that phenazopyridine was predicted (using ABSOLV) to be the least likely molecule to penetrate the blood–brain barrier (Table 2). The molecules predicted most likely to penetrate the barrier are yangonin and desmethoxyyangonin, both of which possess no hydrogen-bond donor groups. Table 2 suggests that such effects are not apparent from comparisons of the calculated octanol–water partition coefficients.

Although hydrogen-bonding is suspected, the definitive causes of the changes in permeability between filter coatings containing 2% phosphatidylcholine in dodecane and those containing only dodecane are not well understood. No evidence of precipitation was seen in any of the solutions used in the filter-IAM assay. In the case of phenazopyridine, water solubility effects can be ruled out, even though this molecule has high octanol–water log *P*. The predicted solubility using ABSOLV is 200 μg/ml (Table 2). We measured the solubility of the compound at pH 7.4 to be 15 μg/ml (unpublished). The donor and acceptor well concentrations of phenazopyridine were ~5 μg/ml, well below the solubility limit. Given the interesting PAMPA results reported recently by Wohnsland and Faller (2001), where filters were coated only with an alkane, the effects of phospholipid additives need to be more thoroughly investigated.

For LC–MS detection, two concerns were allayed in the course of this study. The first issue was the general applicability of LC–MS. Because electrospray ionization response is varied from compound to compound, generic conditions had to be used, and it was hoped that these conditions would be amenable to at least 80% of the compounds tested. It should be noted that in addition to the kava samples, the other test compounds were selected on the basis of their permeability characteristics, and not for the applicability to LC–MS. Nonetheless, Table 4 shows that these conditions were appropriate for over 95% of the compounds investigated.

The second concern was linearity of response, since electrospray ionization is most linear at very low concentration levels and does not enjoy the dynamic range of UV detection. The worst-case scenario would be compounds of very low permeability. In this case, the donor-plate sample would be close to the starting concentration, while the acceptor-plate levels would be several orders of magnitude lower. Since permeability coefficients are derived from raw peak area ratios of donor/acceptor samples, a non-linear response would result in numbers which were significantly different than those obtained by direct UV detection. Fortunately, this was not the case.

In the determination of diffusion rates across a filter-bound artificial membrane, LC–MS can offer a complementary approach to UV detection. While UV detection offers quick results due to parallel detection of all samples, LC–MS offers the advantages: cassette samples to increase analytical throughput, confirmation of molecular weights, characterization of impurities, and measuring compounds that have no UV chromophore. By using an LC–MS system for quantitation of compounds from the PSR4p system, these requisite analyses can be performed as part of the absorption modeling process, and some time can be saved by the use of cassette dosing, where appropriate.

5. List of abbreviations and symbols

C_A, C_D	Aqueous solute concentration on the acceptor and donor sides of a membrane, respectively (mol cm^{-3})
C_0	Aqueous concentration of the uncharged species (mol cm^{-3})
$C_m(x)$	Solute concentration inside a membrane (mol cm^{-3}), at position x
D_m	Diffusivity of a solute inside a membrane (cm^2 s^{-1})

filter-IAM	Filter-immobilized artificial membranes technique for assessing membrane permeability
h	Membrane thickness (cm)
J	Flux across a membrane (mol cm^2 s^{-1})
K_p	Membrane/water partition coefficient
PAMPA	Parallel artificial membrane permeability assay
P_0	Intrinsic artificial membrane permeability (cm s^{-1}), i.e. permeability of the uncharged form of solute
P_e	Effective artificial-membrane permeability (cm s^{-1})
pK_a	Ionization constant (negative log form)
ΣC_a, ΣC_d	Sum of hydrogen bond acceptor and donor factors, respectively, estimated by HYBOT [20] from a 2D structure of a molecule; $C_a > 0$ and $C_d < 0$. The Gibbs free energy of a hydrogen-bond is estimated to be $2.5\ C_aC_d + 5.7$ (kJ mol^{-1}).

Acknowledgements

*p*ION is grateful for the support received from Wyeth-Ayerst and Hoffmann-La Roche through a consortium for the development of the high-throughput instrument and the associated methodologies. *p*ION also thanks Manfred Kansy (Roche) for many stimulating discussions concerning permeability measurements. This work was supported in part by the United States Department of Agriculture, Agricultural Research Service Specific Cooperative Agreement No. 58-6408-7-012. The authors are grateful for the technical assistance from Konstantin Tsinmann, Cynthia M. Berger, Chau Du, Deren Dohoda (*p*ION), Beverly Kenney (Waters), and Karl J. Box (Sirius Analytical Instruments, UK).

References

Abraham, M.H., Chadha, H.S., Mitchell, R.C., 1994. Hydrogen bonding. 33. Factors that influence the distribution of solutes between blood and brain. J. Pharm. Sci. 83, 1257–1268.

Avdeef, A., Bucher, J.J., 1978. Accurate measurements of the concentration of hydrogen ions with a glass electrode: calibrations using the Prideaux and other universal buffer solutions and a computer-controlled automatic titrator. Anal. Chem. 50, 2137–2142.

Avdeef, A., 2001. High-throughput solubility measurements. In: Testa, B., van de Waterbeemd, H., Folkers, G., Guy, R. (Eds.), Pharmacokinetic Optimization in Drug Research: Biological, Physicochemical and Computational Strategies. Helvetica Chimica Acta and Wiley–VCH, Zurich and Weinheim, pp. 305–326.

Backhaub, C., Krieglstein, J., 1992. Extracts of kava (*Piper methysticum*) and its methysticum constituents protect brain tissue against ischemic damage in rodents. Eur. J. Pharmacol. 215, 265–269.

Bruneton, J., 1995. In: Pharmacognosy, Phytochemistry, Medicinal Plants. Lavoisier, Paris, p. 263.

Furgiuele, A.R., Kinnard, W.J., Aceto, M.M., 1965. Central activity of aqueous extracts of *Piper methysticum* (Kava). J. Pharm. Sci. 54, 247–252.

Ganzera, M., Khan, I.A., 1999. Analytical techniques for the determination of lactones in *Piper methysticum* Forst. Chromatographia 50, 649–653.

Holm, E., Staedt, U., Heep, J., 1991. Profile of the neurophysiological effects of dl-kavain: cerebral sites of action and sleep–wakefulness rhythm in animals. Arzneim.-Forsch. 41, 673–683.

Kansy, M., Senner, F., Gubernator, K., 1998. Physicochemical high throughput screening: parallel artificial membrane permeation assay in the description of passive absorption processes. J. Med. Chem. 41, 1007–1010.

Kilham, C., 1996. In: Kava: Medicine Hunting in Paradise. Park Street Press, Rochester, p. 55.

Leung, A.Y., Foster, S., 1996. In: Encyclopedia of Common Natural Ingredients Used in Food, Drugs, and Cosmetics. Wiley, New York, p. 330.

Palm, K., Luthman, K., Ros, J., Gråsjo, J., Artursson, P., 1999. Effect of molecular charge on intestinal epithelial drug transport: pH-dependent transport of cationic drugs. J. Pharmacol. Exp. Ther. 291, 435–443.

Raevsky, O.A., Fetisov, V.I., Trepalina, E.P., McFarland, J.W., Schaper, K.-J., 2000. Quantitative estimation of drug absorption in humans for passively transported compounds on the basis of their physico-chemical parameters. Quant. Struct.-Act. Relatsh. 19, 366–374.

Rothen-Rutishauser, B., Braun, A., Günthert, M., Wunderli-Allenspach, H., 2000. Formation of multilayers in the caco-2 cell culture model: a confocal laser scanning microscopy study. Pharm. Res. 17, 460–465.

Sawada, G.A., Barsuhn, C.L., Lutzke, B.S., Houghton, M.E., Padbury, G.E., Ho, N.F.H., Raub, T.J., 1999. Increased lipophilicity and subsequent cell partitioning decrease passive transcellular diffusion of novel, highly lipophilic antioxidants. J. Pharmacol. Exp. Ther. 288, 1317–1326.

Singh, Y.N., 1992. Kava: an overview. J. Ethnopharmacol. 37, 13–45.

Thompson, M., Lennox, R.B., McClelland, R.A., 1982. Structure and electrochemical properties of microfiltration filter-lipid membrane systems. Anal. Chem. 54, 76–81.

Weiss, T.F., 1996. In: Transport. Cellular Biophysics, Vol. I. MIT Press, Cambridge, MA, pp. 83–183.

Wils, P., Warnery, A., Phung-Ba, V., Legrain, S., Scherman, D., 1994. High lipophilicity decreases drug transport across intestinal epithelial cells. J. Pharmacol. Exp. Ther. 269, 654–658.

Wohnsland, F., Faller, B., 2001. High-throughput permeability pH profile and high-throughput alkane/water log *P* with artificial membranes. J. Med. Chem. 44, 923–930.